Absorption of Water by Room-Temperature Ionic Liquids: Effect of Anions on Concentration and State of Water

CHIEU D. TRAN,* SILVIA H. DE PAOLI LACERDA, and DANIEL OLIVEIRA

Department of Chemistry, Marquette University, P.O. Box 1881, Milwaukee, Wisconsin 53201

Near-infrared (NIR) spectrometry was successfully used for the noninvasive and *in situ* determination of concentrations and structure of water absorbed by room-temperature ionic liquids (RTILs). It was found that RTILs based on 1-butyl-3-methylimidazolium, namely, $[BuMIm]^+[BF_4]^-$, $[BuMIm]^+$[bis((trifluoromethyl)sulfonyl)amide, or $Tf_2N]^-$ and $[BuMIm]^+[PF_6]^-$, are hydroscopic and can quickly absorb water when they are exposed to air. Absorbed water interacts with the anions of the RTILs, and these interactions lead to changes in the structure of water. Among the RTILs studied, $[BF_4]^-$ provides the strongest interactions and $[PF_6]^-$ the weakest. In 24 hours, $[BuMIm]^+[BF_4]^-$ can absorb up to 0.320 M of water, whereas $[BuMIm]^+[PF_6]^-$ can only absorb 8.3×10^{-2} M of water. It seems that higher amounts of water can be absorbed when the anion of the RTIL can strongly interact and hence stabilize absorbed water molecules by forming hydrogen bonds with them or inducing hydrogen bonds among water molecules. More importantly, the NIR technique can be sensitively used for the noninvasive, *in situ* determination of absorbed water in RTILs, without any pretreatment, and at limits of detection as low as 3.20×10^{-3} M.

Index Headings: **Room-temperature ionic liquids; Green chemistry; Near-infrared; Acousto-optic tunable filter.**

INTRODUCTION

Room-temperature ionic liquids (RTILs) are a group of organic salts that are liquid at room temperature.[1,2] They have unique chemical and physical properties including air and moisture stablity, high solubility power, and virtually no vapor pressure. Because of these properties, they can serve as a ''green'' recyclable alternative to the volatile organic compounds that are traditionally used as industrial solvents.[1–4] In fact, RTILs have been successfully used as solvents in many applications including organic and inorganic syntheses,[5–7] chemical separations,[8–16] and electrochemistry.[17,18]

Room-temperature ionic liquids are known to be hydroscopic and can absorb significant amounts of water from the atmosphere.[19–22] Properties of RTILs, including their solubility, polarity, viscosity, and conductivity, are not only changed by but also are dependent on the amount of absorbed water.[1,19–22] As a consequence, absorbed water may alter rates of chemical reactions and efficiencies of various processes in RTILs. It is, therefore, of particular importance that a method capable of determining concentrations and molecular states of absorbed water be developed. Such considerations have prompted a variety of studies including those based on the use of FT-IR to determine molecular states of water in RTILs and on fluorescence techniques to determine the effect of water on the polarity of RTILs.[19–22] Unfortunately, these studies are not suited for the direct determination of absorbed water. This may be due to the lack of a suitable technique that has noninvasive and *in situ* capabilities without any pretreatment of samples. Near-infrared (NIR) spectrometry can offer a solution to this problem.

Near-infrared spectrometry has been used extensively in recent years for chemical analysis and characterization[23] because it has many advantages, including wide applicability, noninvasiveness, nondestructiveness, and real-time and on-line capabilities. The NIR region covers the overtone and combination transitions of the C–H, O–H, and N–H groups, and since all organic and most inorganic compounds possess at least one or more of these groups, the technique can, in principle, be used for analysis of all organic and most inorganic compounds. Additionally, because it has real-time and on-line capabilities that satisfy one of twelve principles of Green Chemistry,[24] the NIR technique is suited as a *Green Method.* Unfortunately, in spite of its potentials, to date, the NIR technique has not been used for the determination of water absorbed by RTILs. The limitation is probably due to the fact that both water and RTILs absorb NIR light, and hence, there is extensive overlap among their spectra. High-quality NIR spectra are, therefore, required for subsequent data treatment including background subtraction, deconvolution, and analysis by multivariate methods. A high-performance NIR spectrometer with high sensitivity, high light throughput, high stability, and no drift is needed to measure such spectra. Such a spectrometer was successfully constructed in our laboratory using the acousto-optic tunable filter.[25–27]

An acousto-optic tunable filter (AOTF) is an all-solid-state, electronic dispersive device that is based on the diffraction of light by acoustic waves in an anisotropic crystal.[28–30] The wavelength of the diffracted light is dependent on the frequency and the power of the applied acoustic wave. The scanning speed of the AOTF is defined by the speed of the acoustic wave in the crystal, which is on the order of microseconds. As a consequence, compared to conventional gratings, the AOTFs have such advantages as being all solid state (contains no moving parts), having rapid scanning ability (μs), wide spectral tuning range, and high throughput, and giving high resolution (<1 nm).[28–30] The filters can also provide a unique means to maintain the intensity of the light source (by controlling either the frequency or the power of the applied radio frequency (RF) signal through a feed-back loop).[28–30] As a consequence of this development, an NIR spectrophotometer based on the AOTF is very sensitive, has high light throughput, high stability, and no drift. In fact, we recently developed an AOTF-based NIR spectrometer and successfully used it for a variety of spectroscopic and analytical measurements, including the deter-

Received 17 July 2002; accepted 2 October 2002.

* Author to whom correspondence should be sent.

0003-7028/03/5702-0152$2.00/0

mination of sequences of peptides synthesized by solid-phase combinatorial method and association constants of the inclusion complex formation between cyclodextrins and aromatic compounds, and as the detector for flow injection analysis.[25,27,31]

The information presented is indeed provocative and clearly demonstrates that it is possible to use the AOTF-based NIR spectrometer to determine concentrations and molecular states of water in RTILs. Such consideration prompted us to initiate this study, which aims to use the NIR technique to determine water absorbed by different RTILs including RTIL based on 1-butyl-3-methylimidazolium ($[BMIm]^+$) with different anions such as chloride, $[BF_4]^-$, $[PF_6]^-$, and bis(trifluoromethyl) sulfonyl amide, or $[Tf_2N]^-$.

EXPERIMENTAL

1-Butyl-3-methylimidazolium chloride ($[BuMIm]^+[Cl]^-$) was synthesized according to procedures previously reported.[32] Specifically, it was prepared by mixing equal molar freshly vacuum-distilled 1-methylimidazole and freshly vacuum-distilled *n*-butyl chloride in a round-bottomed flask equipped with a reflux condenser and dried tube and reacting them for 72 h at 90 °C. The resulting viscous liquid was allowed to cool to room temperature and was then washed three times with dried ethyl acetate (3 × 100 mL). The ethyl acetate layer was decanted. Any ethyl acetate remaining in the ionic liquid was removed by evacuating the ionic liquid under vacuum at 70 °C overnight. The final ionic liquid was kept either under nitrogen or vacuum to protect it from moisture. 1-Butyl-3-methylimidazolium tetrafluoroborate ($[BuMIm]^+[BF_4]^-$), 1-butyl-3-methylimidazolium hexafluorophosphate ($[BuMIm]^+[PF_6]^-$), and 1-butyl-3-methylimidazolium bis-(trifluoromethyl)sylfonyl amide ($[BuMIm]^+[Tf_2N]^-$) were prepared from $[BuMIm]^+[Cl]^-$ by metathesis using methods reported previously.[33–35] The final ionic liquids were dried under vacuum at 70 °C overnight and kept either under nitrogen or a vacuum desicator to protect them from moisture. Hydranal, a pyridine-free Karl Fischer reagent (Riedel-de Haen, St. Louis, MO) were used for titration to determine concentrations of water in three ionic liquids. No water was detected in any of the three ionic liquids.[36]

Care was taken to prepare standard samples for the determination of water in the ionic liquids to avoid possible error from water absorbed by the samples from air. Specifically, a sample of an ionic liquid was placed in a 5-mm-pathlength cell with a stopper. If needed, an appropriate amount of deionized, distilled water was promptly added to the cell by a syringe, and the cell with the stopper in place was then vigorously shaken to facilitate dissolution of water. For kinetic determination of absorption of water, a sample of the ionic liquid was placed in the cell without a stopper. The open cell was then placed in the spectrometer, and the spectrometer was programmed to record a set of spectra as a function of time at a specific time interval. NIR spectra were taken on a home-built NIR spectrometer based on an AOTF. Information on the AOTF-based NIR spectrometer was described in detail in our previous papers.[11,12] Normally, each spectrum was an average of 30 spectra taken at 1-nm intervals from 1450 to 2450 nm. Humidity and temperature were measured with a thermometer/hydrometer (RadioShack Corp). The *Origin* program was used to deconvolute spectra into individual bands.

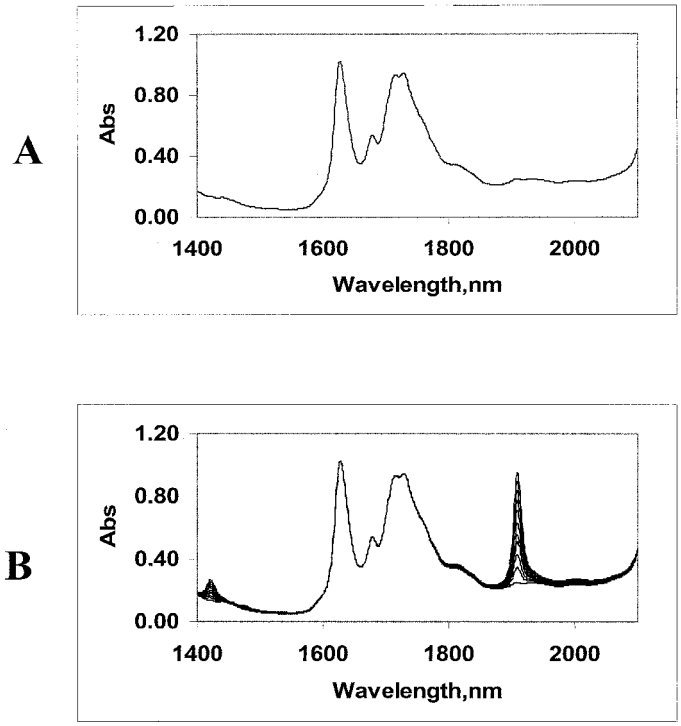

FIG. 1. (**A**) Spectrum of 1-butyl-3-methylimidazolium hexafluorophosphate ($[BuMIm]^+[PF_6]^-$) RTIL in an 0.5-cm-pathlength cell; (**B**) spectra of $[BuMIm]^+[PF_6]^-$ with different concentrations of added water (from bottom to top: 0.000, 0.037, 0.074, 0.111, 0.148, 0.185, 0.221, 0.258, 0.295, 0.332, and 0.368 M).

RESULTS AND DISCUSSION

The NIR spectrum of dried $[BuMIm]^+[PF_6]^-$ ionic liquid is shown in Fig. 1A. The ionic liquid exhibits several bands at 1638, 1719, and 2150 nm and a cluster of bands at >2200 nm. The 1719 nm band and the cluster of bands at >2200 nm (not shown) can be attributed to the overtones and combinations of the aliphatic C–H groups. Overtones and combination transitions of the aromatic C–H groups may be responsible for bands at 1638 and 2150 nm (not shown).

Different amounts of water (from 0.000 to 0.368 M) were added to the dried $[BuMIm]^+[PF_6]^-$ sample and their spectra were recorded (Fig. 1B). A new band at 1910 nm was produced when water was added, and the intensity of this band increases concomitantly with the increase in the concentration of added water. This band can be attributed to the overtone and combination transitions of the O–H groups of water. In addition to this new major band, there seem to be several smaller bands in the region from 1400 to 1500 nm. Clearer observation can be obtained when the background contribution of the $[BuMIm]^+[PF_6]^-$ ionic liquid was subtracted from the spectra shown in Fig. 1B. The resulting spectra, shown in Fig. 2A, clearly show the major O–H band at 1910 nm and several smaller bands from 1400 to 1500 nm. These smaller bands can also be attributed to the overtone transitions of the O–H.

Near-infrared spectra of $[BuMIm]^+[Tf_2N]^-$ and

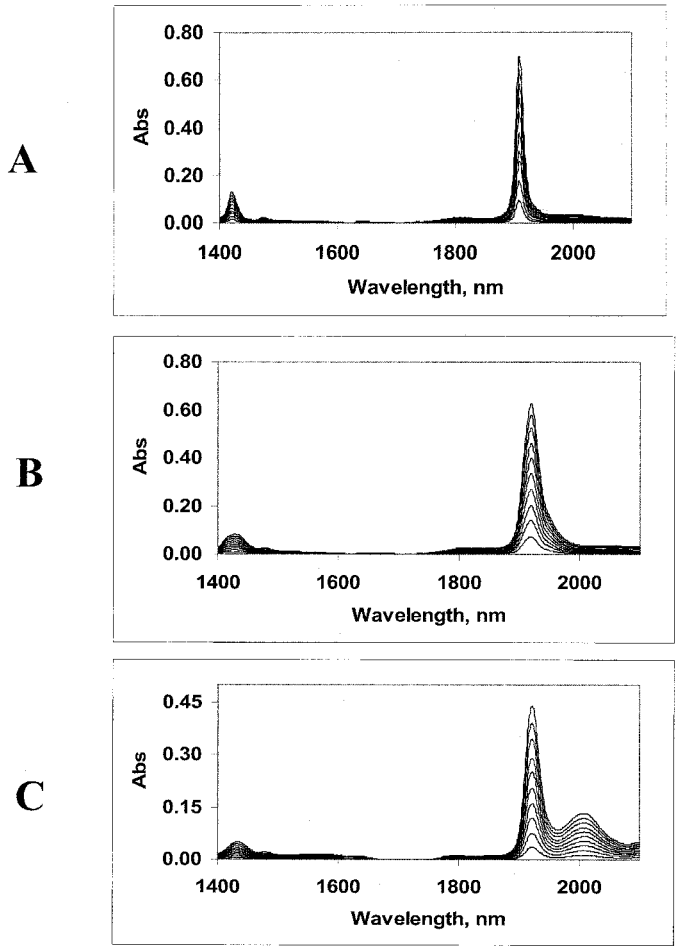

FIG. 2. Spectra of (**A**) $[BuMIm]^+[PF_6]^-$ with 0.000, 0.037, 0.074, 0.111, 0.148, 0.185, 0.221, 0.258, 0.295, 0.332, and 0.368 M of added water; (**B**) $[BuMIm]^+[Tf_2N]^-$ with 0.000, 0.031, 0.061, 0.092, 0.122, 0.153, 0.183, 0.214, 0.244. 0.275, and 0.305 M of added water; and (**C**) $[BuMIm]^+[BF_4]^-$ with 0.000, 0.035, 0.070, 0.105, 0.139, 0.174, 0.209, 0.244, 0.278, 0.313, and 0.347 M of added water. Background absorption of the ionic liquids were removed in these spectra.

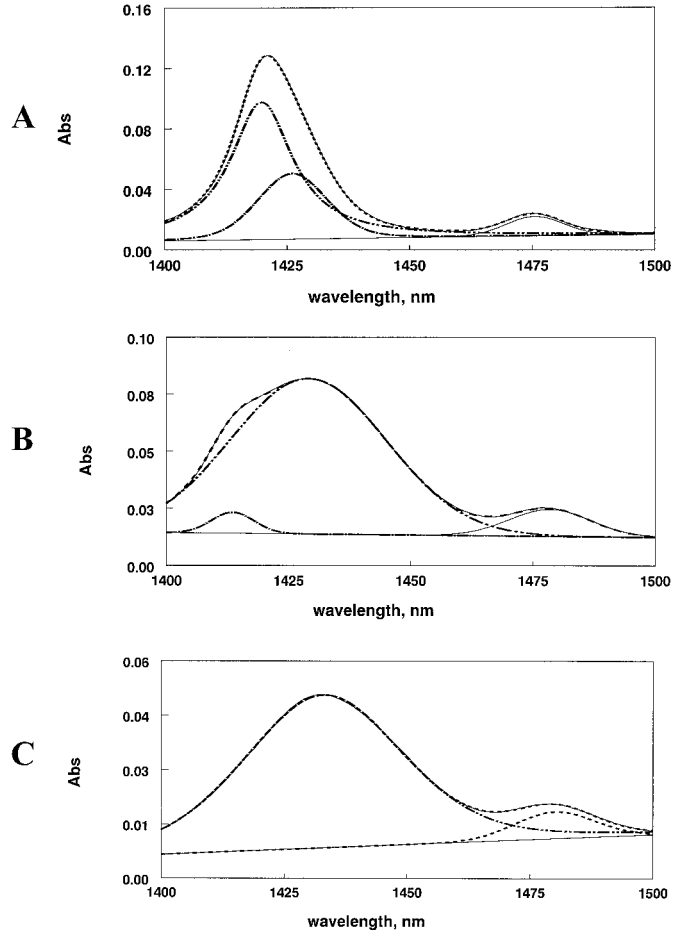

FIG. 3. Deconvoluted spectra in the region from 1400 to 1500 nm for (**A**) $[BuMIm]^+[PF_6]^-$, (**B**) $[BuMIm]^+[Tf_2N]^-$, and (**C**) $[BuMIm]^+[BF_4]^-$.

$[BuMIm]^+[BF_4]^-$ with different amounts of water (from 0.000 to 0.305M for $[BuMIm]^+[Tf_2N]^-$ and 0.000 to 0.347 M for $[BuMIm]^+[BF_4]^-$) were also taken and are shown in Figs. 2B and 2C, respectively (background contribution of the ionic liquids were removed from these spectra). Similar to the $[PF_6]^-$ ionic liquid, adding water to these ionic liquids also led to the generation of the O–H bands. Interestingly, the shape, position, and relative intensity of the O–H bands are found to be strongly dependent on the ionic liquids. The changes are evident in Fig. 3, which plots spectra of highest concentrations of added water (0.37, 0.31, and 0.35 M) in $[BuMIm]^+[PF_6]^-$, $[BuMIm]^+[Tf_2N]^-$, and $[BuMIm]^+[BF_4]^-$, respectively. As illustrated, the single major O–H band at 1909 nm in $[BuMIm]^+[PF_6]^-$ not only became relatively broader but also undewent a red-shift to 1919 nm in $[BuMIm]^+[Tf_2N]^-$ (Figs. 2B and 3). The major O–H band in $[BuMIm]^+[BF_4]^-$ was also red-shifted to 1921 nm. Interestingly, in addition to this band, there is also a new band at 2009 nm (Fig. 2C). The shape and relative intensity of several small bands in the 1400 to 1500 nm region also changed.

It is evident that interactions between water and ionic liquids are strongly dependent on anions of the ionic liquids. It seems that water interacts strongly with the anions, and thus the strength of the interactions is dependent on the anions. These interactions lead to changes in the structure of water, and as a consequence, the structure of water will be different in different ionic liquids. In fact, bands in the 1400–1500 nm region can be resolved into several individual bands. As shown in Fig. 3A, in this region, the spectrum of $[BuMIm]^+[PF_6]^-$ can be resolved into three bands with peaks at 1419, 1426, and 1475 nm. The band at 1419 nm is largest while that at 1475 nm is smallest. Similarly, the spectrum of $[BuMIm]^+[Tf_2N]^-$ can also be resolved into three bands (Fig. 3B), but in this case the last band, which is at about 1478 nm, is relatively larger than the first band at 1414 nm. Conversely, only two bands (1433 and 1479 nm) (Fig. 3C) can be resolved for $[BuMIm]^+[BF_4]^-$. According to previous study,[37] these bands can be attributed to different water species, namely, bands at 1412 and 1491 nm represent two major water species (more than 99%) with weaker and stronger hydrogen bonds, respectively.[37] The third band at around 1438 nm can be attributed to the minor third species that has very small impact on the overall structural dynamics.[37] Since the intensity of the 1419 nm band is relatively higher than that of the 1475 nm band for $[BuMIm]^+[PF_6]^-$ while the reverse is true for

TABLE I. Molar absorptivities of major O–H transitions in different room-temperature ionic liquids.

Ionic liquid	Wavelength, nm	Molar absorptivity, M^{-1} cm^{-1}
$[BuMIm]^+[PF_6]^-$	1421	0.88
	1909	4.97
$[BuMIm]^+[Tf_2N]^-$	1428	0.50
	1919	4.10
$[BuMIm]^+[BF_4]^-$	1432	0.28
	1921	2.48

$[BuMIm]^+[Tf_2N]^-$, and the 1419 nm band is absent in $[BuMIm]^+[BF_4]^-$, the results seem to suggest that among ionic liquids, water forms the strongest hydrogen bonds in $[BuMIm]^+[BF_4]^-$ and the weakest in $[BuMIm]^+[PF_6]^-$.

Molar absorptivities for different bands of water in different ionic liquids were calculated from the spectra shown in Figs. 2A–2C and the values obtained are listed in Table I. These spectra were also used to construct calibration curves for the determination of limits of detection (LOD), which is defined as the amount of water in a RTIL that yielded a signal three times the standard deviation of the blank. LOD values were calculated to be 7.50×10^{-3} M, 3.20×10^{-3} M, and 8.50×10^{-3} M for $[BuMIm]^+[PF_6]^-$, $[BuMIm]^+[Tf_2N]^-$, and $[BuMIm]^+[BF_4]^-$ at 1421, 1428, and 1921 nm, respectively.

As expected, concentrations of water in the ionic liquids as determined by the NIR method agree very well with those obtained using the Karl Fischer titration method. For example, for samples of $[BuMIm]^+[Tf_2N]^-$ containing 9.0×10^{-2} and 0.145 M of water, concentrations determined by the NIR method were $(8.7 \pm 0.4) \times 10^{-2}$ M and 0.150 ± 0.004 M, respectively, while those determined by the Karl Fischer method were 9.0×10^{-2} and 0.140 M, respectively. While it seems that the sensitivity and accuracy of the NIR method is comparable to that of the Karl Fischer method, the former method is superior to the latter method as it is noninvasive and can be used for *in situ* and real-time determination of water in the ionic liquids.

The stopper of the cuvette containing dried $[BuMIm]^+[PF_6]^-$ ionic liquid (Fig. 1A) was then removed, and spectra of the sample were measured every 2 min for the first hour, every 10 min for the next two hours, and every 30 min for the subsequent 21 hours. The spectra obtained are shown in Fig. 4 (for clarity, only spectra taken every 30 min were plotted and background absorption by the ionic liquid was subtracted from these spectra). As illustrated, exposing the ionic liquid to the atmosphere (at 25 °C and 40% humidity) led to the generation of a major band at 1909 nm and two smaller bands in the 1400 to 1500 nm region. The longer the ionic liquid was exposed to air, the higher were the intensities of these bands. Since these bands are identical to the O–H bands of water shown in Figs. 2A and 3A, it is evident that $[BuMIm]^+[PF_6]^-$ ionic liquid absorbed water from the air. Similar measurements were also made on $[BuMIm]^+[Tf_2N]^-$ and $[BuMIm]^+[BF_4]^-$. As expected, exposing these ionic liquids to air led to the generation of new O–H bands whose intensity is increased concomitantly with the increase in exposure time (spectra not shown). It is evident that all of the ionic liquids are very hydroscopic. They absorbed water quickly when they were exposed to air.

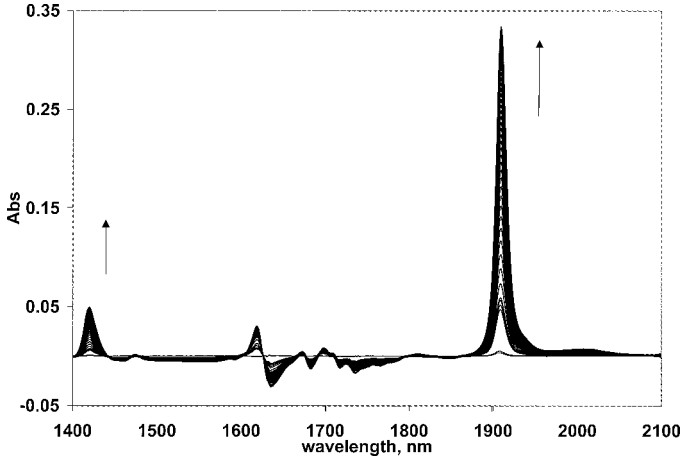

FIG. 4. Changes in NIR spectra of the $[BuMIm]^+[PF_6]^-$ sample when it was exposed to air for 24 h. Spectra were taken every 30 min, and background contribution from the ionic liquid was removed.

Additional information on the absorption processes could be obtained when changes in absorbance of the O–H band in $[BuMIm]^+[PF_6]^-$, $[BuMIm]^+[Tf_2N]^-$, and $[BuMIm]^+[BF_4]^-$ at 1909, 1919, and 1921 nm, respectively, were plotted as a function of time (Fig. 5). It is interesting to observe that at the beginning ($t < 900$ min) $[BuMIm]^+[PF_6]^-$ and $[BuMIm]^+[Tf_2N]^-$ absorb water faster (and hence more) than $[BuMIm]^+[BF_4]^-$. However, their absorption leveled off while that of $[BuMIm]^+[BF_4]^-$ continuously increased. According to this figure, after 24 h, $[BuMIm]^+[BF_4]^-$ should absorb much more water than $[BuMIm]^+[PF_6]^-$ and $[BuMIm]^+[Tf_2N]^-$ and that total amounts of water absorbed by the latter two ionic liquids should be very similar. At the beginning, absorption of water seems to be dependent on the viscosity and diffusion of the ionic liquids, and because the viscosity of $[BuMIm]^+[BF_4]^-$ is much higher (0.20 mPa s) than those of $[BuMIm]^+[PF_6]^-$ and $[BuMIm]^+[Tf_2N]^-$ (0.15 mPa s),[38] water is absorbed by the latter two ionic liquids much faster than the former. However, the thermodynamic factor may become more important since more water was absorbed, namely, faster and more water was absorbed by $[BuMIm]^+[BF_4]^-$ because this ionic liquid can stabilize absorbed water by readily forming stronger hydrogen bonds with its anion.

It is important to point out that the kinetics of water absorption by all ionic liquids are not simple, but relatively complex. They were found to not follow first-order, pseudo-first-order, or second-order rates. This is as expected, as it is known that the physical properties, namely, polarity and viscosity, of the ionic liquids are dependent on the concentration of absorbed water. Furthermore, as results presented in previous sections show, the ionic liquids and their anions interact strongly with water, and the structures of the ionic liquids as well as of water are dependent on the concentration of water. Because the NIR technique measures combination and overtone absorptions of the O–H group, any change in the structure of water would undoubtedly lead to changes in the ab-

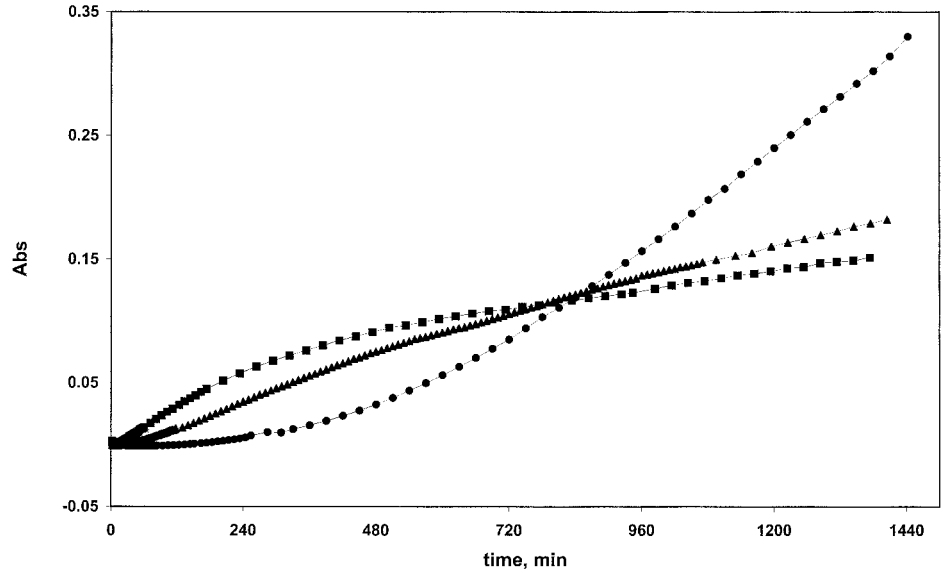

FIG. 5. Changes in absorbance of O–H groups of water plotted as a function of time for $[BuMIm]^+[BF_4]^-$ (●), $[BuMIm]^+[Tf_2N]^-$ (■), and $[BuMIm]^+[PF_6]^-$ (▲).

sorption of the O–H group. Therefore, the kinetics of water absorption may not follow a simple first-order reaction but may undergo changes in the order as the reaction proceeds.

Using the molar absorptivity values listed in Table I, concentrations of water absorbed by these ionic liquids after being exposed to air for 24 h were calculated to be 0.320, 0.097, and 0.083 M for $[BuMIm]^+[BF_4]^-$, $[BuMIm]^+[Tf_2N]^-$, and $[BuMIm]^+[PF_6]^-$, respectively. The order of absorbed water concentrations is correlated to the strength of the hydrogen bonding among water molecules and also to the strength of the interaction between water and the anions of the ionic liquids. This is hardly surprising, as it is expected that higher amounts of water can be absorbed when absorbed water is stabilized by readily forming stronger hydrogen bonds among themselves as well as with the anions of the ionic liquids.

In summary, it has been demonstrated that near-infrared spectrometry (NIR) is particularly suited for the noninvasive and *in situ* determination of concentrations and structure of water absorbed by RTILs. Results from the NIR study show, for the first time, that RTILs based on 1-butyl-3-methylimidazolium, namely, $[BuMIm]^+[BF_4]^-$, $[BuMIm]^+[Tf_2N]^-$, and $[BuMIm]^+[PF_6]^-$, are hydroscopic and quickly absorb water when they are exposed to air. It was found that absorbed water interacts with the anions of the RTILs, and these interactions lead to changes in the structure of water. Among the RTILs studied, $[BF_4]^-$ provides the strongest interactions and $[PF_6]^-$ the weakest. In a given time, the amount of absorbed water is highest in $[BuMIm]^+[BF_4]^-$ and lowest in $[BuMIm]^+[PF_6]^-$. It seems that higher amounts of water can be absorbed when the anion of the RTIL can strongly interact with, and hence stabilize, absorbed water molecules by forming hydrogen bonds with them or inducing hydrogen bonds among water molecules. More importantly, the NIR technique can be sensitively used for the noninvasive, *in situ* determination of absorbed water in RTILs, without any pretreatment, and at limits of detection as low as 1.60×10^{-3} M. Because of its noninvasiveness, sensitivity, and fast scanning ability, NIR is particularly suited for the determination of the kinetics of absorption of water by RTILs. This is, in fact, the subject of our current intense investigation.

1. T. Welton, Chem. Rev. **99,** 2071 (1999).
2. A. E. Visser, R. P. Swatloski, and R. D. Rogers, Green Chemistry, Feb. 1 (2001).
3. J. S. Wilkes and M. J. Zaworotko, Chem. Commun. 965 (1992).
4. J. G. Huddleston, H. D. Willauer, R. P. Swatloski, and R. D. Rogers, Chem. Commun. 1765 (1998).
5. R. C. Buijsman, E. V. Vuuren, and J. G. Serrenburg, Org. Lett. **3,** 3785 (2002).
6. J. M. Fraile, J. I. Garcia, C. I. Herrerias, J. A. Mayoral, and M. Carrie, Tetrahedron: Asymmetry **12,** 1891 (2002).
7. M. M. Anna, V. Gallo, P. Mastrorilli, C. F. Nobile, G. Romanazzi, and G. P. Suranna, Chem. Commun. 434 (2002).
8. M. L. Dietz and J. A. Dzielawa, Chem. Commun. 2124 (2001).
9. L. A. Blanchard, D. Hancu, E. J. Beckman, and J. F. Brennecke, Nature (London) **399,** 28 (1999).
10. L. A. Blanchard and J. F. Brennecke, Ind. Eng. Chem. Res. **40,** 287 (2001).
11. S. G. Kazarian, B. J. Briscoe, and T. Welton, Chem. Commun. 2047 (2000).
12. D. W. Armstrong, L. K. Zhang, L. He, and M. L. Gross, Anal. Chem. **73,** 3679 (2001).
13. D. W. Armstrong, L. He, and Y. S. Liu, Anal. Chem. **71,** 3873 (1999).
14. A. Berthod, H. He, and D. W. Armstrong, Chromatographia **53,** 63 (2001).
15. M. Vaher, M. Koel, and M. Kaljurand, Electrophoresis **23,** 426 (2002).
16. E. G. Yanes, S. R. Gratz, M. J. Baldwin, S. E. Robinson, and A. M. Stalcup, Anal. Chem. **73,** 3838 (2001).
17. D. L. Compton and J. A. Laszlo, J. Electroanal. Chem. **520,** 71 (2002).
18. B. M. Quinn, Z. Ding, R. Moulton, and A. J. Bard, Langmuir **18,** 1734 (2002).
19. K. A. Fletcher and S. Pandey, Appl. Spectrosc. **56,** 266 (2002).
20. S. N. V. K. Aki, J. Brennecke, and A. Samanta, Chem. Commun. 413 (2001).
21. S. G. Kazarian, B. J. Briscoe, and T. Welton, Chem. Commun. 2047 (2000).
22. L. Cammarata, S. G. Kazarian, P. A. Salter, and T. Welton, Phys. Chem. Chem. Phys. **3,** 5192 (2001).
23. D. A. Burns and E. W. Ciurczak, *Handbook of Near-Infrared Analysis* (Marcel Dekker, New York, 1992).

24. P. T. Anastas and J. C. Warner, *Green Chemistry: Theory and Practice* (Oxford University Press, Oxford, 1998).
25. M. J. Politi, C. D. Tran, and G. H. Gao, J. Phys. Chem. **99,** 14137 (1995).
26. C. D. Tran and X. Kong, Anal. Biochem. **286,** 67 (2000).
27. T. Alexander and C. D. Tran, Anal. Chem. **73,** 1062 (2001).
28. C. D. Tran, Anal. Chem. **64,** 971A (1992).
29. C. D. Tran, Talanta **45,** 237 (1997).
30. C. D. Tran, Anal. Lett. **33,** 1711 (2000).
31. M. S. Baptista, C. D. Tran, and G. H. Gao, Anal. Chem. **68,** 971 (1996).
32. J. S. Wilkes, J. A. Levisky, R. A. Wilson, and C. L. Hussey, Inorg. Chem. **21,** 1263 (1982).
33. J. D. Holbrey and K. R. Seddon, J. Chem. Soc., Dalton Trans. 2133 (1999).
34. J. G. Huddleston, H. D. Willauer, R. P. Swatloski, A. E. Visser, and R. D. Rogers, Chem. Commun. 1765 (1998).
35. P. Bonhote, A. P. Dias, N. Papageourgiou, K. Kalyanasundaram, and M. Gratzel, Inorg. Chem. **35,** 1168 (1996).
36. E. Scholz, *Karl Fischer Titration* (Springer Verlag, New York, 1984).
37. V. H. Segtnan, Š. Šašic, T. Isaksson, and Y. Ozaki, Anal. Chem. **73,** 3153 (2001).
38. A. Noda, K. Hayamizu, and M. Watanabe, J. Phys. Chem. B **105,** 4603 (2001).